Desalination and Water Treatment
www.deswater.com
doi: 10.1080/19443994.2015.1110841

57 (2016) 20904–20914
September

Taylor & Francis
Taylor & Francis Group

Sequestration of Ni(II) onto graphene oxide from synthetic wastewater as affected by coexisting constituents

Xue Li[a,*], Mei Yu[b], Qingmei Lv[a], Yongsheng Tan[b]

[a]*College of Yuanpei, Shaoxing University, Shaoxing 312000, People's Republic of China, Tel. +86 13858480289; email: lixue.213@usx.edu.cn (X. Li), Tel. +86 18069515189; email: 10631834@qq.com (Q. Lv)*
[b]*Department of Physics, Shaoxing University, Shaoxing 312000, People's Republic of China, Tel. +86 13857590690; email: 1688465@qq.com (M. Yu), Tel. +86 13675731833; email: tanysh@usx.edu.cn (Y. Tan)*

Received 27 May 2015; Accepted 17 October 2015

ABSTRACT

This article examines the sequestration of Ni(II) onto graphene oxide (GO) by an adsorption process using batch technique. The role of contact time, medium pH, and coexisting constituents like humic acid (HA) and/or fulvic acid (FA) in the adsorption of Ni(II) onto GO was studied. The results indicated that the adsorption of Ni(II) onto GO increased from ~20 to ~95% at pH 2.0–9.0, and then maintained the high level with increasing pH. Kinetic data showed that the adsorption obtained equilibrium quickly and was fitted well by the pseudo-second-order equation. The presence of HA/FA imposing a positive role Ni(II) adsorption onto GO was found at pH < 8.0, whereas a negative role in the adsorption of Ni (II) onto GO was observed at pH > 8.0. The thermodynamic analysis from the temperature-dependent adsorption isotherms suggests that the adsorption of Ni(II) onto GO is spontaneous and endothermic. Experimental results provided evidence that the adsorption of Ni(II) onto GO was mainly attributed to surface complexation. These findings indicate that GO is a suitable material in the solidification and immobilization of Ni(II) from aqueous solutions in the wastewater treatment.

Keywords: Sequestration; Ni(II); Graphene oxide; Coexisting constituents

1. Introduction

The contamination of groundwater and surface water by toxic organic substance, heavy metals, and/or radionuclides has been increasingly an important issue due to their great hazardous to human being and environmental ecology. So, it is very necessary to find effective methods to remediate these toxic contaminants [1–12]. Among these contaminants, nickel (Ni(II)) is a non-biodegradable toxic heavy metal ion that is widely present in wastewater. The main source of Ni(II) in wastewater is from industrial production processes including mining, galvanization, batteries manufacturing, smelting, and so on [12–20]. The accumulation of Ni(II) in the natural water environment has a toxic effect on living species. So, it is of crucial importance to remove Ni(II) from wastewaters before discharging into the environment [12–20]. Generally, adsorption is an economical and efficient technique and has been widely utilized to treat Ni(II) from wastewaters. In this respect, a wide range of

*Corresponding author.

adsorbents with good adsorption capacity such as mordenite [13], Na-attapulgite [14], diatomite [15,16], Na-rectorite [17], GMZ bentonite [18], titanate nanotubes [19], and carbon nanotube [20] have been reported as nice adsorbents for nickel ion removal from aqueous solutions. However, researches concerning to investigating novel potential adsorbents for the removal of metal ions with much higher adsorption capacities and efficiencies are always necessary.

Graphene (G) and graphene oxide (GO), a new member in carbon family, have attracted interdisciplinary investigations due to the outstanding properties [21–25]. Recently, G and GO have aroused researchers' widespread attentions as potential adsorbents and showed an outstanding capability for the removal of various inorganic and organic contaminants [25–35]. For instance, Zhao et al. [26,28] found that GO showed strong adsorption capacity to heavy metal ions such as Pb(II), Cd(II), and Co(II), and the extent of O-containing functional groups is mainly responsible for the adsorption of heavy metal ions. Ramesha et al. [29] applied G and GO as effective adsorbents toward anionic and cationic dyes. Wang et al. [32] investigated the adsorption behavior of polycyclic aromatic hydrocarbons by G and GO nanosheets. Pei et al. [35] studied the adsorption capacity of 1,2,4-trichlorobenzene, 2,4,6-trichlorophenol, 2-naphthol, and naphthalene on G and GO. All these investigations indicated that both G and GO possess higher adsorption capacity and better regeneration and reusability characteristics than commercial adsorbents did, suggesting that G and GO can be used to remediate a wide range of organic and inorganic contaminants in wastewater treatment. However, to the best of our knowledge, there is little information with respect to the simultaneous removal of heavy metal ions and organics [36]. Nevertheless, we should realize that heavy metals and organics may exist simultaneously at many contaminated sites. For example, the presence of humic acid (HA) and/or fulvic acid (FA) may influence the adsorption of heavy metals onto GO. Therefore, it is significant to study the adsorption of heavy metals onto GO in the presence of organics and vice versa.

Therefore, in this study, we devote to the sequestration of Ni(II) onto GO from synthetic wastewater, and the role of coexisting constituents in the adsorption were studied in detail. The main objectives are as follows: (1) to investigate the adsorption kinetics and to simulate the data with a pseudo-second-order equation; (2) to study the adsorption of Ni(II) onto GO by varying conditions, viz. pH, foreign ions, HA/FA; (3) to presume the adsorption mechanism of Ni(II) onto GO.

2. Materials and methods

2.1. Materials and chemicals

All chemicals used in the experiments were purchased in analytical purity and used without any purification. All solutions were prepared with deionized water. Ni(II) stock solution (1,000 mg/L) was prepared as follows: 0.10 g nickel metal powder (purity > 99.9%) was dissolved in 10 mL of 3.0 mol L^{-1} HNO_3 and then shifted to a 100-mL volumetric flask. The stock solution was diluted with deionized water to obtain standard solutions with different concentrations. HA and FA were extracted from the soil of Hua-Jia county (Gansu province, China) and had been characterized in detail previously using cross-polarization magic angle spinning (CPMAS), ^{13}C NMR spectra, and potentiometric titration methods [37–39]. GO was prepared using the modified Hummers method and was characterized, which has been described in detail in our previous report [25].

2.2. Adsorption methods

The adsorption experiments were conducted in the polyethylene test tubes under ambient conditions using the batch technique. The stock solution of GO and $NaNO_3$ solution was first contacted for 24 h to obtain the equilibration between GO and $NaNO_3$. Then, Ni(II) stock solution and HA/FA solution were added to obtain the desired concentrations of different constituents. Negligible amount of 0.01 mol L^{-1} HNO_3 or NaOH was added to achieve the desired pH. The samples were gently shaken for 24 h to achieve adsorption equilibration and centrifuged, and then the supernatant was filtered using 0.45-μm membrane filters to separate the solid from liquid phases. The concentration of Ni(II) in solution was analyzed by atomic absorption spectrometer (AA-6300C, Shimadzu). The amount of Ni(II) adsorbed onto GO was calculated from the difference between the initial concentration and the equilibrium concentration. All the experimental data were the averages of duplicate determinations. The average uncertainties were ~5%.

3. Results and discussion

3.1. Characterization of GO

The results of the FT-IR and scanning electron microscope (SEM) characterization of the prepared GO are shown in Fig. 1. The oxygen-containing functional groups on GO were characterized by FTIR analysis (Fig. 1(A)). Different functional groups are found in the FTIR spectrum, i.e. C–O group at 1,073 cm^{-1}, C=O group at 1,628 cm^{-1}, C=C group at 1,377 and

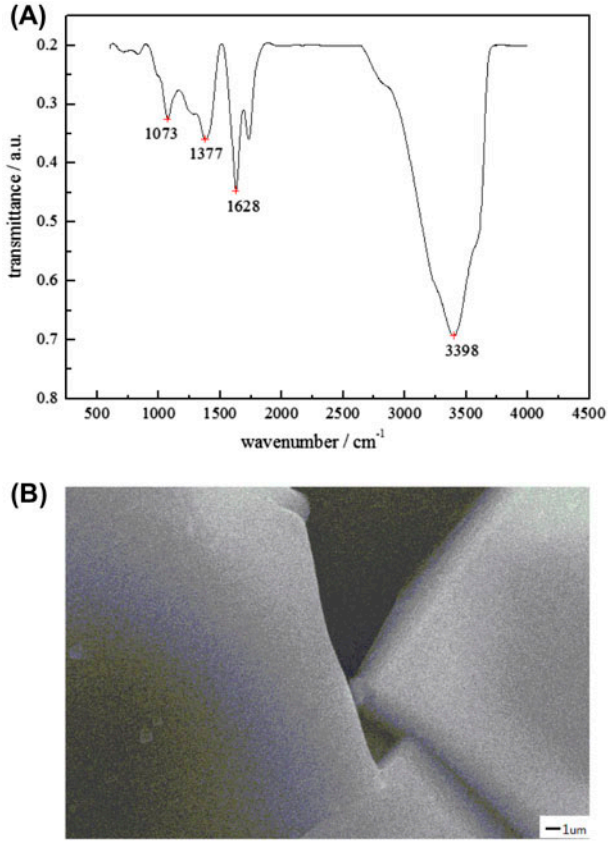

Fig. 1. FTIR spectrum (A) and typical SEM (B) of GO.

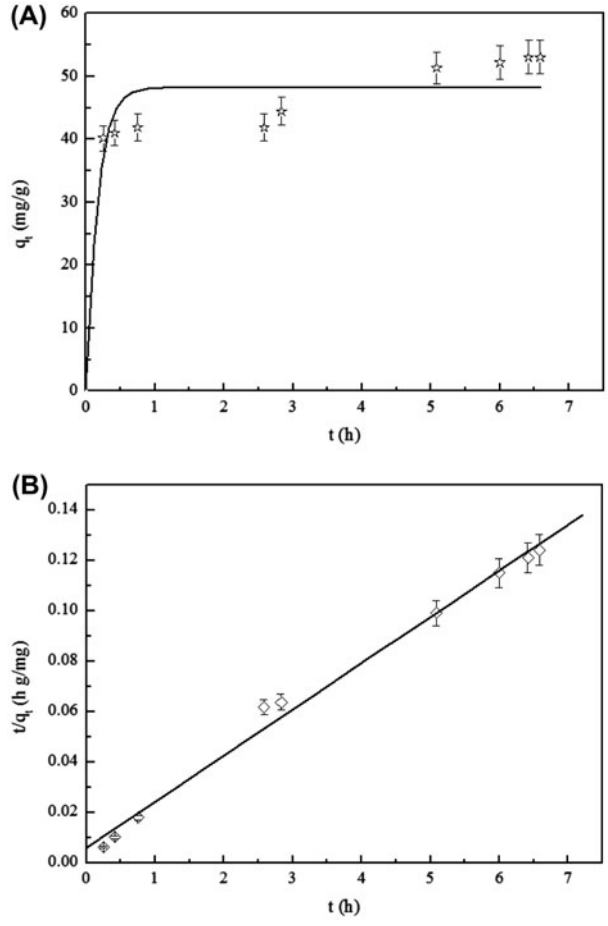

Fig. 2. (A) The role of contact time in Ni(II) adsorption onto GO and (B) pseudo-second-order rate calculation of Ni(II) adsorption onto GO, pH 5.0 ± 0.1, T = 293 K, m/V = 0.1 g L^{-1}, $C_{(NaNO_3)}$ = 0.01 mol L^{-1}, $Ni(II)_{initial}$ = 15 mg L^{-1}.

3,398 cm^{-1}, which indicates that large amounts of oxygen-containing functional groups exist on GO. SEM (Fig. 1(B)) shows that GO exist in loose state, the surface is smooth, edge part because there was a crimp in fold oxidation state.

3.2. The role of contact time

The role of contact time in Ni(II) adsorption onto GO is shown in Fig. 2(A). One can see that 2 h is enough to obtain equilibrium for Ni(II) adsorption onto GO under our experimental conditions, indicating that chemical interaction rather than physical interaction is responsible for the adsorption of Ni(II) onto GO [16,25]. So, in the other experiments, we select 24 h in order to achieve the adsorption equilibrium. Besides, the pseudo-second-order rate equation is utilized to fit the kinetic adsorption process of Ni(II) onto GO [20,25]:

$$\frac{t}{q_t} = \frac{1}{2kq_e^2} + \frac{1}{q_e}t \quad (1)$$

where q_t (mg g^{-1}) is the amount of Ni(II) adsorbed onto GO at time t (h), q_e (mg g^{-1}) is the equilibrium adsorption capacity, and k (g mg^{-1} h^{-1}) is the pseudo-second-order rate constant of adsorption. A linear plot of t/q_t vs. t is achieved (Fig. 2(B)). The values of k and q_e calculated from the slopes and intercepts of the kinetic equation are listed in Table 1. The correlation coefficient of the pseudo-second-order rate equation is ~1.0, suggesting that the kinetic equation can be well simulated by the pseudo-second-order model.

3.3. The role of pH and ionic strength

Fig. 3(A) shows the results of the pH-dependence of Ni(II) adsorption onto GO in the presence of 0.001, 0.01, or 0.1 mol L^{-1} $NaNO_3$ solution, respectively. It is clear that solution pH plays an important role in the adsorption of Ni(II) onto GO. The removal of Ni(II)

Table 1
Kinetic parameters of Ni(II) adsorption onto GO

	Pseudo-second-order parameters		
C_0 (Ni(II)) (mg L^{-1})	q_e (mg g^{-1})	k (g mg^{-1} h^{-1})	R^2
15	54.555	0.0291	0.9920

from solution onto GO increases gradually from ~20% to ~95% with solution pH increasing from 2.0 to 10.0, and then the adsorption maintains high level with increase in pH. The results are consistent with the adsorption of Ni(II) onto a range of other adsorbents such as mordenite [13], Na-attapulgite [14], diatomite [16], Na-rectorite [17], GMZ bentonite [18], titanate nanotubes [19], and carbon nanotube [20]. The increase in Ni(II) adsorption onto GO with increase in pH is mainly resulted from the hydrolysis of Ni(II) and the surface properties of GO. Fig. 3(B) shows the relative proportion of Ni(II) species calculated from the hydrolysis constants of Ni(II). It is clear that Ni(II) presents in the species of Ni^{2+}, $Ni(OH)^+$, $Ni(OH)_2^0$, $Ni(OH)_3^-$, and $Ni(OH)_4^{2-}$ as a function of pH [16,19]. At pH < 9.0, the main specie is Ni^{2+}. So, the low Ni^{2+} adsorption is partly attributed to the competition between H^+/Na^+ and Ni^{2+} on GO surface sites. Besides, the zeta potential of GO becomes negative due to the deprotonation reaction ($GO-OH \rightarrow GO-O^- + H^+$) with increase in pH, which leads to the adsorption of Ni^{2+} to the deprotonated surface of GO. The point of zero charge (pH_{pzc}) of GO was measured to be at pH ~ 4.0 [25]. So, At pH < pH_{pzc}, the surface charge of GO is positive, and ion exchange interaction between Ni^{2+} and H^+/Na^+ on GO results in the adsorption of Ni^{2+}. Besides, at pH > pH_{pzc}, the positively charged Ni^{2+} can be easily adsorbed on the negatively charged GO, and thus the adsorption of Ni (II) onto GO increases with increase in pH.

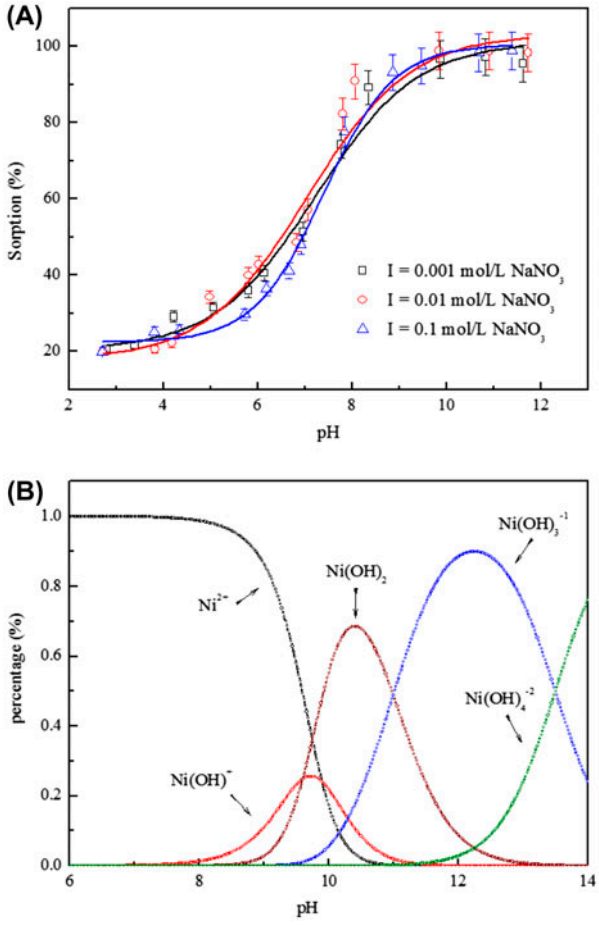

Fig. 3. (A) The role of pH and ionic strength in Ni(II) adsorption onto GO, T = 293 K, m/V = 0.1 g L^{-1}, $C_{(NaNO_3)}$ = 0.01 mol L^{-1}, $Ni(II)_{initial}$ = 15 mg L^{-1} and (B) relative proportion of Ni(II) species as a function of pH.

Fig. 3(A) also shows the role of the coexisting electrolyte concentration in Ni(II) adsorption onto GO in wide pH range, and we can see that ionic strength effect is fairly negligible. The coexisting electrolyte can affect the thickness and potential of the double layer at the GO/water interface, thus influencing the binding of Ni(II) species onto GO surface. The coexisting electrolytes are occupied at the same plane as the outer-sphere complex that is expected to be more susceptible to ionic strength variations than inner-sphere complexes. Therefore, the adsorption of Ni(II) onto GO was mainly attributed to the formation of inner-sphere complex. It was proposed by Hayes and Leckie [40] that the role of coexisting electrolytes in the adsorption of Ni(II) onto GO can be used to predict the mechanism. The coexisting electrolytes-independent and pH-dependent adsorption is mainly inner-sphere complexation, while the coexisting electrolytes-dependent and pH-dependent adsorption is mainly outer-sphere complexation. Consequently, we can see that the adsorption of Ni(II) onto GO is inner-sphere surface complexation, which is due to the strong interaction of Ni(II) with the O-containing functional groups on GO (Fig. 4).

3.4. The role of HA/FA

Fig. 5 shows the pH-dependent of Ni(II) adsorption onto GO in the absence and presence of HA/FA. We can see from Fig. 5 that HA/FA showed a positive role in Ni(II) adsorption onto GO at pH < 8.0, while HA/FA showed a negative role in Ni(II) adsorption onto GO at pH > 8.0. The adsorption of HA and FA onto GO as a function of pH was determined in our

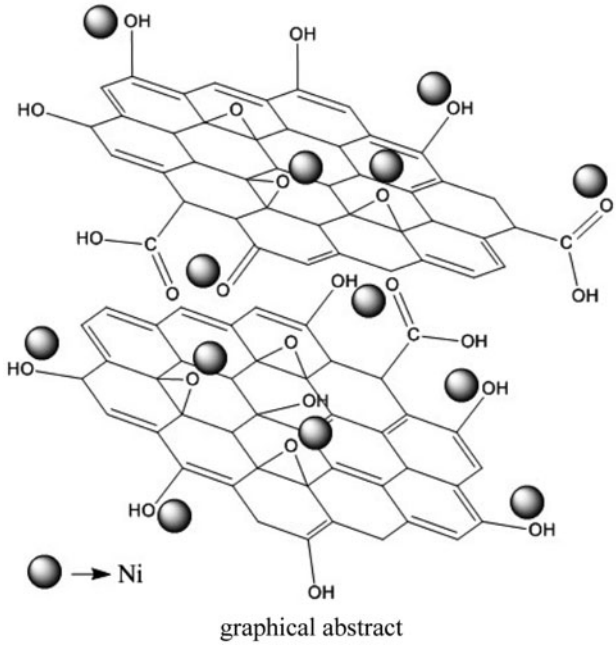

Fig. 4. The strong interaction of Ni(II) with the O-containing functional groups on GO.

previous work [25], and it was found that ~90% of HA/FA can be adsorbed on GO at low pH, and then the adsorption decreases with pH increasing. It was reported that both HA and FA were negatively charged at pH 3.0–10.0 [15,19,41]. So, at pH < 8.0, the negatively charged HA/FA can be easily adsorbed onto the positively charged GO surface as a result of electrostatic attraction, resulting in the enhancement of Ni(II) adsorption onto GO due to the strong complexation ability of surface adsorbed HA/FA with Ni(II).

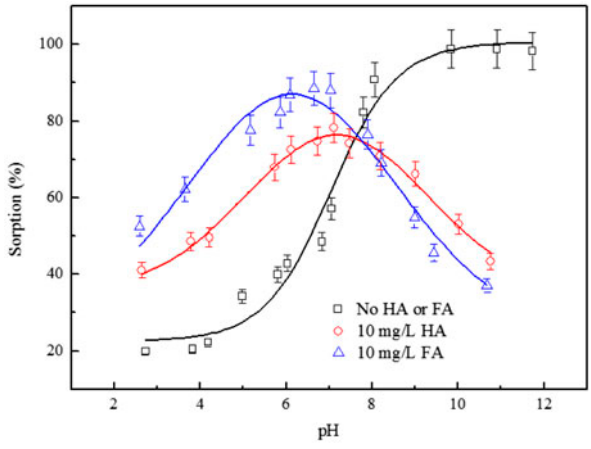

Fig. 5. The role of HA/FA in Ni(II) adsorption onto GO, T = 293 K, m/V = 0.1 g L^{-1}, $C_{(NaNO_3)}$ = 0.01 mol L^{-1}, $Ni(II)_{initial}$ = 15 mg L^{-1}.

However, at pH > 8.0, it is very difficult for the negatively charged HA/FA to be adsorbed onto the negatively charged GO surface due to the electrostatic repulsion, hence, the HA/FA in solution forms HA/FA-Ni(II) soluble complexes, and thereby the adsorption of Ni(II) onto GO was greatly reduced. In previous investigations, Fan et al. [14] studied sorption of Ni(II) to Na-attapulgite in the absence and presence of humic substances; Yang et al. [42] studied HA/FA effects on sorption behavior of Ni(II) uptake mechanisms on mordenite surfaces; Hu et al. [43] studied the impact of HA/FA on sorption behavior of radionuclide Ni(II) in illite–water suspensions; Xu et al. [44] studied adsorption of Ni(II) on Na-montmorillonite in the absence/presence of HA; and Sheng et al. [45] studied HA/FA effects of Ni(II) sorption to MnO_2. These results are similar to those of previous work.

3.5. The role of coexistent electrolyte ions

Fig. 6 shows the adsorption of Ni(II) onto GO as affected by different coexistent electrolyte ions, viz. Li^+, Na^+, K^+, ClO_4^-, NO_3^-, and Cl^-, respectively. The selection of these ions has been made due to their wide presence in the natural groundwater and industrial wastewaters. From Fig. 6(A), we can see that the role of anions in Ni(II) adsorption onto GO is in the order of $Cl^- > NO_3^- \sim ClO_4^-$ at pH < 8.0. The nature of the counter-ions, destined to stabilize Ni(II) ions in the cationic form, can also influence their adsorption onto GO. The ionic radius of the anions is $Cl^- < NO_3^- \sim ClO_4^-$ and the anion with smaller radius may form complexes with the oxygen-containing functional groups on GO, hence Ni(II) adsorption onto GO decreases. Besides, compared with NO_3^- and ClO_4^-, Cl^- is easier to form idiocratic adsorption onto GO surface, changing the surface state of GO and decreases the availability of binding sites [18,46]. The result is consistent with the sorption of Pb(II) on diatomite [46]. However, the role of coexistent cations in the adsorption of Ni(II) onto the surface of GO from solution was negligible in the entire pH range (Fig. 6(B)).

3.6. Adsorption isotherms of Ni(II) onto GO and thermodynamic study

The adsorption isotherms of Ni(II) onto the surface of GO at 293, 313, and 333 K are shown in Fig. 7. It can be seen from Fig. 6 that the adsorption isotherm of Ni(II) onto GO is the highest at T = 333 K and is the lowest at T = 293 K. The result indicates that high temperature is advantageous for the adsorption of Ni(II)

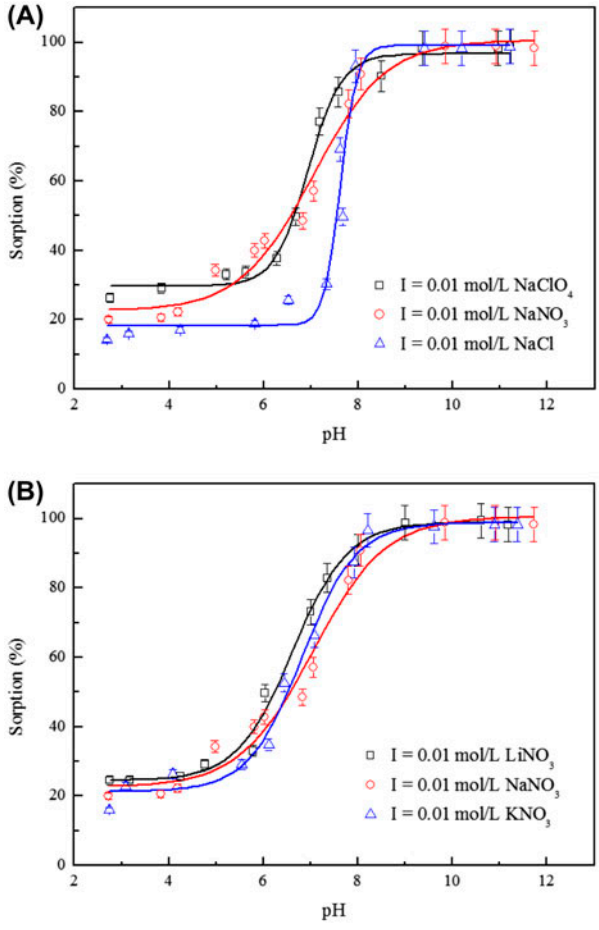

Fig. 6. The role of coexistent electrolyte anions (A) and cations (B) in Ni(II) adsorption onto GO, T = 293 K, m/V = 0.1 g L^{-1}, $Ni(II)_{initial}$ = 15 mg L^{-1}.

onto GO. Several factors may be responsible for the increase in Ni(II) adsorption onto GO with the increase in temperature. Increased diffusion rate of Ni (II) into GO pores due to increased temperature may contribute to the observed adsorption. The increase in reaction temperature may result in the increase in proportion and activity of Ni(II) ions in solution, the affinity of Ni(II) ions to GO surface, or the charge and the potential of GO surface [43,47]. For isotherm modeling, herein, the linear model, Langmuir, Freundlich, and D–R isotherms are conducted to fit the adsorption isotherms of Ni(II) onto GO and to establish the relationship between the amount of Ni(II) adsorbed onto GO and the concentration of Ni(II) remained in solution.

The Langmuir isotherm has been used to characterize monolayer adsorption process. Its form can be represented as:

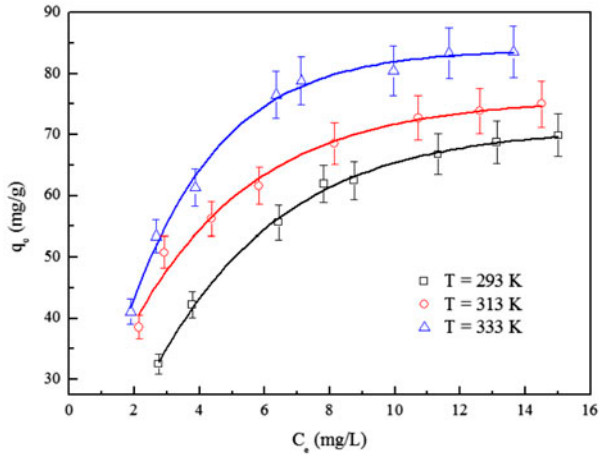

Fig. 7. Adsorption isotherms of Ni(II) onto GO at three different temperatures, pH 5.0 ± 0.1, T = 293 K, m/V = 0.1 g L^{-1}.

$$q = \frac{bq_{max}C_{eq}}{1 + bC_{eq}} \tag{2}$$

which can be expressed in the linear form as:

$$\frac{C_{eq}}{q} = \frac{1}{bq_{max}} + \frac{C_{eq}}{q_{max}} \tag{3}$$

where C_{eq} (mol L^{-1}) is the equilibrium concentration of Ni(II), q (mol g^{-1}) is the amount of Ni(II) adsorbed on per weight unit of GO, q_{max} (the maximum adsorption capacity, mol g^{-1}) is the amount of Ni(II) at complete monolayer coverage, b (L mol^{-1}) is a constant that relates to the heat of adsorption [43,47,48]. The Freundlich isotherm is based on the adsorption phenomenon occurred onto a heterogeneity surface. It has the following form:

$$q = K_F C_{eq}^{n} \tag{4}$$

which can be expressed in linear form as:

$$\log q = \log K_F + n \log C_{eq} \tag{5}$$

where K_F (mol^{1-n} L^n g^{-1}) represents the adsorption capacity when Ni(II) equilibrium concentration equals to 1, and n represents the degree of adsorption dependence [47,48]. The D–R isotherm can be used to describe adsorption on both homogeneous and heterogeneous surfaces, which has the form:

$$q = q_{max} \exp(-\beta\varepsilon^2) \tag{6}$$

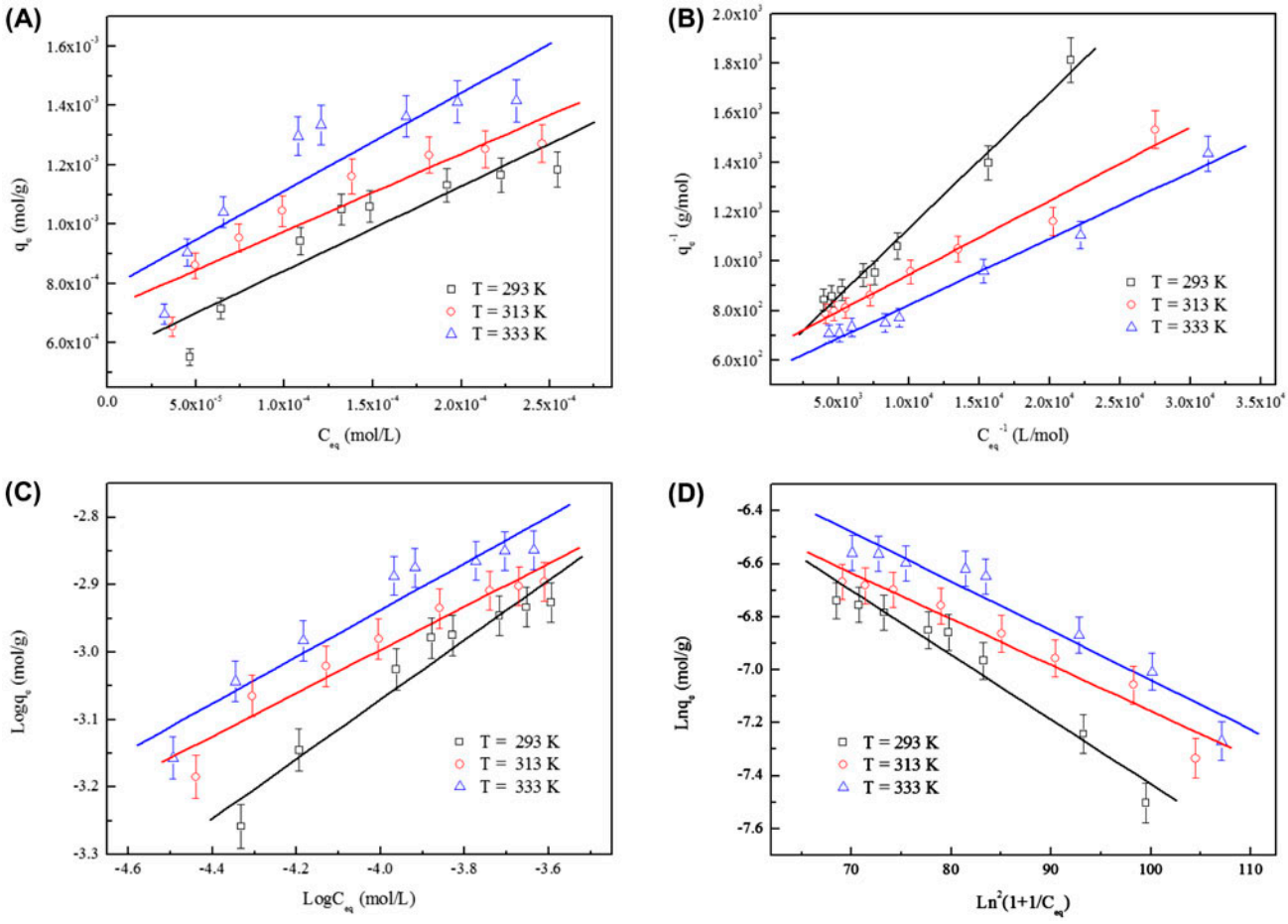

Fig. 8. Fitting results of (A) linear, (B) Langmuir, (C) Freundlich, and (D) D–R adsorption isotherms of Ni(II) adsorption onto GO at three different temperatures.

$$\ln q = \ln q_{\max} - \beta\varepsilon^2 \tag{7}$$

where q and $q_{\max}$ are defined above; β (mol^2 kJ^{-2}) is the activity coefficient related to the mean adsorption energy; ε is the Polanyi potential, which is equal to:

$$\varepsilon = RT \ln\left(1 + \frac{1}{C_{eq}}\right) \tag{8}$$

where R (8.3145 J mol^{-1} K^{-1}) is ideal gas constant. T (K) is the absolute temperature in kelvin. E (kJ mol^{-1}) is defined as the free energy change, which requires to transfer 1 mol of Ni(II) from solution to GO. The relation is given as:

$$E = \frac{1}{\sqrt{2\beta}} \tag{9}$$

Adsorption of Ni(II) onto GO simulated by the models is shown in Fig. 8(A)–(D), respectively. The relative parameters calculated from the models are listed in Table 2. From the correlation coefficients, we can conclude that the Langmuir isotherm model simulated the experimental data better than other isotherm models. The value of K_F calculated from the Freundlich isotherm model is large, indicating that GO has a high adsorption affinity toward Ni(II). The deviation of n from unity suggests a nonlinear adsorption of Ni(II) on the heterogeneous surfaces of GO. The magnitude of E is useful for estimating the mechanism of the adsorption, which is dominated by chemical interaction if E is in the range of 8.0–16.0 kJ mol^{-1}, whereas physical forces may affect the adsorption in the case of $E < 8.0$ kJ mol^{-1} [43]. The E values for Ni(II) adsorption onto the surface of GO are 11.03 kJ mol^{-1} at 293 K, 13.94 kJ mol^{-1} at 313 K, 14.31 kJ mol^{-1} at 333 K, respectively, which are in the adsorption energy range

Table 2
The parameters for linear, Langmuir, Freundlich, and D–R isotherms of Ni(II) adsorption onto GO at different temperatures

Linear model	A	B	R^2
T = 293 K	2.855	5.577×10^{-4}	0.8466
T = 313 K	2.611	7.149×10^{-4}	0.8557
T = 333 K	3.296	7.844×10^{-4}	0.7925
Langmuir model	q_{max} (mol g^{-1})	b (L mol^{-1})	R^2
T = 293 K	1.711×10^{-3}	1.063×10^{4}	0.9872
T = 313 K	1.544×10^{-3}	2.165×10^{4}	0.9723
T = 333 K	1.803×10^{-3}	2.062×10^{4}	0.9840
Freundlich model	K_F (mol^{1-n} L^n g^{-1})	n	R^2
T = 293 K	4.990×10^{-2}	0.4421	0.9389
T = 313 K	1.924×10^{-2}	0.3202	0.9328
T = 333 K	2.817×10^{-2}	0.3468	0.9182

D–R model	q_{max} (mol g^{-1})	β (mol^2 kJ^{-2})	E (kJ mol^{-1})	R^2
T = 293 K	6.777×10^{-3}	4.112×10^{-3}	11.027	0.9509
T = 313 K	4.451×10^{-3}	2.573×10^{-3}	13.940	0.9440
T = 333 K	5.686×10^{-3}	2.441×10^{-3}	14.312	0.9327

Table 3
Comparison of maximum adsorption capacities of different adsorbents for Ni(II)

Sorbent	Maximum adsorption capacity (mg g^{-1})	Refs.
GMZ bentonite	15.69	[18]
Oxidized multi-walled carbon nanotubes	4.17	[20]
Illite	10.27	[43]
MnO_2	34.362	[45]
Lin'an montmorillonite	53.99	[49]
MX-80 bentonite	39.06	[50]
Multi-walled carbon nanotubes	11.67	[51]
GO	113.59	Present work

Table 4
Values of thermodynamic parameters for Ni(II) adsorption onto GO

T (K)	ΔG° (kJ mol^{-1})	ΔS° (J mol^{-1} K^{-1})	ΔH° (kJ mol^{-1})
293	−23.370	118.02	11.228
313	−25.933		11.025
333	−28.091		11.228

of chemical interaction. This suggests that Ni(II) adsorption onto GO is attributed to chemical interaction rather than physical interaction. A comparison as shown in Table 3 of the maximum adsorption capacities of Ni(II) on GO studied in this work with that of other common adsorbents such as oxidized multi-walled carbon nanotubes, MX-80 bentonite, and MnO_2

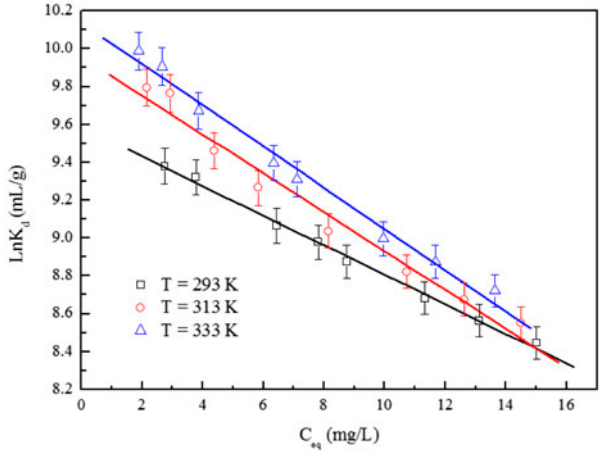

Fig. 9. The linear plot of ln K_d vs. C_{eq} for Ni(II) uptake onto GO at three different temperatures.

Table 5
Recycling for Ni(II) uptake on GO

Run	1	2	3	4	5	6
Adsorption (%)	98.6%	96.2%	94.8%	93.7%	92.1%	90.9%

powders documented in the literature shows that the adsorption capacity of Ni(II) on GO is much higher than that of other common adsorbents. Thus, GO can be used as an alternative material to uptake Ni(II) from aqueous solution.

The thermodynamic parameters (ΔH°, ΔS°, and ΔG°) for Ni(II) adsorption onto GO can be determined from the temperature-dependence adsorption. Free energy change (ΔG°) can be calculated from the relationship:

$$\Delta G^\circ = -RT \ln K^\circ \tag{10}$$

where K° is the equilibrium constant. Values of $\ln K^\circ$ obtained by plotting $\ln K_d$ vs. C_{eq} (Fig. 9) for Ni(II) adsorption onto GO and extrapolating C_{eq} to zero are 9.59 (T = 293 K), 9.96 (T = 313 K), and 10.14 (T = 333 K). Standard entropy change (ΔS°) is calculated from the equation:

$$\left(\frac{\partial \Delta G^\circ}{\partial T}\right)_P = -\Delta S^\circ \tag{11}$$

The average standard enthalpy change (ΔH°) is calculated from the expression:

$$\Delta H^\circ = \Delta G^\circ + T\Delta S^\circ \tag{12}$$

The values obtained are tabulated in Table 4. A positive value of the ΔH° indicates that the adsorption is endothermic. The ΔG° is negative as expected for a spontaneous process under the conditions applied. The value of ΔG° becomes more negative with the increase in temperature, which indicates that the reaction is more favorable at higher temperatures. The positive value of the ΔS° shows some structural changes in GO during the adsorption process, causing an increase in the disorderness of the solid–solution system [43].

3.7. Potential application in actual wastewater

To take into account environmental sustainability and economic efficiency, it is indispensable to adopt renewable material to reduce the wastewater treatment cost. The repeated availability of GO for Ni(II) uptake on GO through many cycles of adsorption/desorption is quite crucial for the application of GO in the removal of Ni(II) from wastewater in real work. At present, the practical recycle and utilization of GO in the immobilization of Ni(II) was studied. We found that the recycling was valid for at least six times as shown in Table 5, to give a satisfied removal percentage even in the sixth round. The experimental results of recycle and utilization illustrate that the GO can be employed repeatedly in Ni(II) uptake.

4. Conclusions

Batch technique was adopted to investigate the adsorption of Ni(II) onto GO as a function of various factors such as contact time, pH, ionic strength, and temperature under ambient conditions. The adsorption increases with pH increasing at pH < 10.0, and then the adsorption maintains high level at pH > 10.0. The adsorption of Ni(II) onto GO is independent on ionic strength, and thus inner-sphere surface complexation is the main mechanism responsible for the adsorption reaction. The presence of HA/FA enhances the adsorption of Ni(II) onto GO at low pH values, while reduces Ni(II) adsorption onto GO at high pH values. The thermodynamic analysis from the temperature-dependent adsorption isotherms suggests that the adsorption of Ni(II) onto GO is spontaneous and endothermic. By integrating all the above-mentioned analysis results together, one can conclude that GO has a great application potential for the cost-effective remediation of Ni(II)-contaminated wastewaters.

Acknowledgments

Financial supports from the National Natural Science Foundation of China (11204180) and the Zhejiang Provincial Natural Science Foundation of China (LQ13A040004) are acknowledged.

References

[1] J.O. Nriagu, J.M. Pacyna, Quantitative assessment of worldwide contamination of air, water and soils by trace metals, Nature 333 (1988) 134–139.

[2] G. Sheng, X. Shao, Y. Li, J. Li, H. Dong, W. Cheng, X. Gao, Y. Huang, Enhanced removal of uranium(VI) by nanoscale zerovalent iron supported on Na–bentonite and an investigation of mechanism, J. Phys. Chem. A 118 (2014) 2952–2958.
[3] W.C. Song, D.D. Shao, S.S. Lu, X.K. Wang, Simultaneous removal of uranium and humic acid by cyclodextrin modified graphene oxide nanosheets, Sci. China Chem. 57 (2014) 1291–1299.
[4] D.D. Shao, J.X. Li, X.K. Wang, Poly(amidoxime)-reduced graphene oxide composites as adsorbents for the enrichment of uranium from seawater, Sci. China Chem. 57 (2014) 1449–1458.
[5] G.D. Sheng, H.P. Dong, Y.M. Li, Characterization of diatomite and its application for the retention of radiocobalt: Role of environmental parameters, J. Environ. Radioact. 113 (2012) 108–115.
[6] X.L. Tan, M. Fang, X.M. Ren, H.Y. Mei, D.D. Shao, X.K. Wang, Effect of silicate on the formation and stability of Ni–Al LDH at the γ-Al_2O_3 surface, Environ. Sci. Technol. 48 (2014) 13138–13145.
[7] G. Sheng, B. Hu, Role of solution chemistry on the trapping of radionuclide Th(IV) using titanate nanotubes as an efficient adsorbent, J. Radioanal. Nucl. Chem. 298 (2013) 455–464.
[8] Y.M. Li, J.F. Li, Y.L. Zhang, Mechanism insights into enhanced Cr(VI) removal using nanoscale zerovalent iron supported on the pillared bentonite by macroscopic and spectroscopic studies, J. Hazard. Mater. 227–228 (2012) 211–218.
[9] G.D. Sheng, H.P. Dong, R.P. Shen, Y.M. Li, Microscopic insights into the temperature-dependent adsorption of Eu(III) onto titanate nanotubes studied by FTIR, XPS, XAFS and batch technique, Chem. Eng. J. 217 (2013) 486–494.
[10] G. Sheng, S. Yang, Y. Li, X. Gao, Y. Huang, X. Wang, Retention mechanisms and microstructure of Eu(III) on manganese dioxide studied by batch and high resolution EXAFS technique, Radiochim. Acta 102 (2014) 155–167.
[11] X.M. Ren, S.T. Yang, F.C. Hu, B. He, J.Z. Xu, X.L. Tan, X.K. Wang, Microscopic level investigation of Ni(II) sorption on Na-rectorite by EXAFS technique combined with statistical *F*-tests, J. Hazard. Mater. 252–253 (2013) 2–10.
[12] X.L. Tan, J. Hu, G. Montavon, X.K. Wang, Sorption speciation of nickel(II) onto Ca-montmorillonite: Batch, EXAFS techniques and modeling, Dalton Trans. 40 (2011) 10953–10960.
[13] S.T. Yang, G.D. Sheng, Z.Q. Guo, X.L. Tan, J.Z. Xu, X.K. Wang, Investigation of radionuclide ^{63}Ni(II) sequestration mechanisms on mordenite by batch and EXAFS spectroscopy study, Sci. China Chem. 55 (2012) 632–642.
[14] Q.H. Fan, D.D. Shao, Y. Lu, W.S. Wu, X.K. Wang, Effect of pH, ionic strength, temperature and humic substances on the sorption of Ni(II) to Na-attapulgite, Chem. Eng. J. 150 (2009) 188–195.
[15] G.D. Sheng, R.P. Shen, H.P. Dong, Y.M. Li, Colloidal diatomite, radionickel, and humic substance interaction: A combined batch, XPS, and EXAFS investigation, Environ. Sci. Pollut. Res. 20 (2013) 3708–3717.
[16] G.D. Sheng, S.T. Yang, J. Sheng, J. Hu, X.L. Tan, X.K. Wang, Macroscopic and microscopic investigation of Ni(II) sequestration on diatomite by batch, XPS, and EXAFS techniques, Environ. Sci. Technol. 45 (2011) 7718–7726.
[17] X.L. Tan, C.L. Chen, S.M. Yu, X.K. Wang, Sorption of Ni^{2+} on Na-rectorite studied by batch and spectroscopy methods, Appl. Geochem. 23 (2008) 2767–2777.
[18] S.T. Yang, J.X. Li, Y. Lu, Y.X. Chen, X.K. Wang, Sorption of Ni(II) on GMZ bentonite: Effects of pH, ionic strength, foreign ions, humic acid and temperature, Appl. Radiat. Isot. 67 (2009) 1600–1608.
[19] G.D. Sheng, L. Ye, Y.M. Li, H.P. Dong, H. Li, X. Gao, Y.Y. Huang, EXAFS study of the interfacial interaction of nickel(II) on titanate nanotubes: Role of contact time, pH and humic substances, Chem. Eng. J. 248 (2014) 71–78.
[20] S.T. Yang, J.X. Li, D.D. Shao, J. Hu, X.K. Wang, Adsorption of Ni(II) on oxidized multi-walled carbon nanotubes: Effect of contact time, pH, foreign ions and PAA, J. Hazard. Mater. 166 (2009) 109–116.
[21] T.A. Duster, J.E.S. Szymanowski, C.Z. Na, A.R. Showalter, B.A. Bunker, J.B. Fein, Surface complexation modeling of proton and metal sorption onto graphene oxide, Colloids Surf., A 466 (2015) 28–39.
[22] G.D. Sheng, Y.M. Li, X. Yang, X.M. Ren, S.T. Yang, J. Hu, X.K. Wang, Efficient removal of arsenate by versatile magnetic graphene oxide composites, RSC Adv. 2 (2012) 12400–12407.
[23] Y.H. Zhang, Y.L. Tang, S.Y. Li, S.L. Yu, Sorption and removal of tetrabromobisphenol A from solution by graphene oxide, Chem. Eng. J. 222 (2013) 94–100.
[24] Y. Li, G.D. Sheng, J. Sheng, Magnetite decorated graphene oxide for the highly efficient immobilization of Eu(III) from aqueous solution, J. Mol. Liq. 199 (2014) 474–480.
[25] X. Li, X.P. Tang, Y.F. Fang, Using graphene oxide as a superior adsorbent for the highly efficient immobilization of Cu(II) from aqueous solution, J. Mol. Liq. 199 (2014) 237–243.
[26] G.X. Zhao, J.X. Li, X.M. Ren, C.L. Chen, X.K. Wang, Few-layered graphene oxide nanosheets as superior Sorbents for heavy metal ion pollution management, Environ. Sci. Technol. 45 (2011) 10454–10462.
[27] S.B. Yang, C.L. Chen, Y. Chen, J.X. Li, D.Q. Wang, X.K. Wang, W.P. Hu, Competitive adsorption of Pb (II), Ni(II) and Sr(II) ions on graphene oxides: A combined experimental and theoretical study, ChemPlusChem. 80 (2015) 480–484.
[28] G.X. Zhao, X.M. Ren, X. Gao, X.L. Tan, J.X. Li, C.L. Chen, Y.Y. Huang, X.K. Wang, Removal of Pb(II) ions from aqueous solutions on few-layered graphene oxide nanosheets, Dalton Trans. 40 (2011) 10945–10952.
[29] G.K. Ramesha, A. Vijaya Kumara, H.B. Muralidhara, S. Sampath, Graphene and graphene oxide as effective adsorbents toward anionic and cationic dyes, J. Colloid Interface Sci. 361 (2011) 270–277.
[30] S.T. Yang, S. Chen, Y.L. Chang, A.N. Cao, Y.F. Liu, H.F. Wang, Removal of methylene blue from aqueous solution by graphene oxide, J. Colloid Interface Sci. 359 (2011) 24–29.
[31] G.X. Zhao, L. Jiang, Y.D. He, J.X. Li, H.L. Dong, X.K. Wang, W.P. Hu, Sulfonated graphene for persistent aromatic pollutant management, Adv. Mater. 23 (2011) 3959–3963.

[32] J. Wang, Z.M. Chen, B.L. Chen, Adsorption of polycyclic aromatic hydrocarbons by graphene and graphene oxide nanosheets, Environ. Sci. Technol. 48 (2014) 4817–4825.
[33] S. Pavagadhi, A.L.L. Tang, M. Sathishkumar, K.P. Loh, R. Balasubramanian, Removal of microcystin-LR and microcystin-RR by graphene oxide: Adsorption and kinetic experiments, Water Res. 47 (2013) 4621–4629.
[34] G.X. Zhao, J.X. Li, X.K. Wang, Kinetic and thermodynamic study of 1-naphthol adsorption from aqueous solution to sulfonated graphene nanosheets, Chem. Eng. J. 173 (2011) 185–190.
[35] Z.G. Pei, L.Y. Li, L.X. Sun, S.Z. Zhang, X.Q. Shan, S. Yang, B. Wen, Adsorption characteristics of 1,2,4-trichlorobenzene, 2,4,6-trichlorophenol, 2-naphthol and naphthalene on graphene and graphene oxide, Carbon 51 (2013) 156–163.
[36] J.H. Deng, X.R. Zhang, G.M. Zeng, J.L. Gong, Q.Y. Niu, J. Liang, Simultaneous removal of Cd(II) and ionic dyes from aqueous solution using magnetic graphene oxide nanocomposite as an adsorbent, Chem. Eng. J. 226 (2013) 189–200.
[37] G.D. Sheng, Q. Yang, F. Peng, H. Li, X. Gao, Y.Y. Huang, Determination of colloidal pyrolusite, Eu(III) and humic substance interaction: A combined batch and EXAFS approach, Chem. Eng. J. 245 (2014) 10–16.
[38] X.L. Tan, Q.H. Fan, X.K. Wang, B. Grambow, Eu(III) sorption to TiO_2 (anatase and rutile): batch, XPS, and EXAFS studies, Environ. Sci. Technol. 43 (2009) 3115–3121.
[39] X.L. Tan, X.K. Wang, H. Geckeis, Th Rabung, Sorption of Eu(III) on humic acid or fulvic acid bound to hydrous alumina studied by SEM-EDS, XPS, TRLFS, and batch techniques, Environ. Sci. Technol. 42 (2008) 6532–6537.
[40] K.F. Hayes, J.O. Leckie, Modeling ionic strength effects on cation adsorption at hydrous oxide/solution interfaces, J. Colloid Interface Sci. 115 (1987) 564–572.
[41] G.D. Sheng, J.X. Li, D.D. Shao, J. Hu, C.L. Chen, Y.X. Chen, X.K. Wang, Adsorption of copper(II) on multiwalled carbon nanotubes in the absence and presence of humic or fulvic acids, J. Hazard. Mater. 178 (2010) 333–340.
[42] S.T. Yang, G.D. Sheng, X.L. Tan, J. Hu, J.Z. Du, G. Montavon, X.K. Wang, Determination of Ni(II) uptake mechanisms on mordenite surfaces: A combined macroscopic and microscopic approach, Geochim. Cosmochim. Acta 75 (2011) 6520–6534.
[43] B.W. Hu, W. Cheng, H. Zhang, S.T. Yang, Solution chemistry effects on sorption behavior of radionuclide ^{63}Ni(II) in illite-water suspensions, J. Nucl. Mater. 406 (2010) 263–270.
[44] D. Xu, X. Zhou, X.K. Wang, Adsorption and desorption of Ni^{2+} on Na-montmorillonite: Effect of pH, ionic strength, fulvic acid, humic acid and addition sequences, Appl. Clay Sci. 39 (2008) 133–141.
[45] G. Sheng, J. Hu, H. Jin, S. Yang, X. Ren, J. Li, Y. Chen, X. Wang, Effect of humic acid, fulvic acid, pH, ionic strength and temperatureon ^{63}Ni(II) sorption to MnO_2, Radiochim. Acta 98 (2010) 1–9.
[46] G.D. Sheng, S.W. Wang, J. Hu, Y. Lu, J.X. Li, Y.H. Dong, X.K. Wang, Adsorption of Pb(II) on diatomite as affected via aqueous solution chemistry and temperature, Colloids Surf., A 339 (2009) 159–166.
[47] B.W. Hu, W. Cheng, H. Zhang, G.D. Sheng, Sorption of radionickel to goethite: Effect of water quality parameters and temperature, J. Radioanal. Nucl. Chem. 285 (2010) 389–398.
[48] G.D. Sheng, Y.M. Li, H.P. Dong, D.D. Shao, Environmental condition effects on radionuclide ^{64}Cu(II) sequestration to a novel composite: Polyaniline grafted multiwalled carbon nanotubes, J. Radioanal. Nucl. Chem. 293 (2012) 797–806.
[49] X.L. Tan, J. Hu, X. Zhou, S.M. Yu, X.K. Wang, Characterization of Lin'an montmorillonite and its application in the removal of Ni^{2+} from aqueous solutions, Radiochim. Acta 96 (2008) 487–495.
[50] D.D. Shao, D. Xu, S.W. Wang, Q.H. Fang, W.S. Wu. Y.H. Dong, X.K. Wang, Modeling of radionickel sorption on MX-80 bentonite as a function of pH and ionic strength. Sci. China Ser. B: Chem. 52 (2009) 362–371.
[51] X.L. Tan, M. Fang, C.L. Chen, S.M. Yu, X.K. Wang, Counterion effects of nickel and sodium dodecylbenzene sulfonate adsorption to multiwalled carbon nanotubes in aqueous solution, Carbon 46 (2008) 1741–1750.